

# Electron Paramagnetic Resonance Study of Pr<sup>4+</sup> Ions Doped in BaHfO<sub>3</sub> Perovskite

Keitaro Tezuka and Yukio Hinatsu

*Division of Chemistry, Graduate School of Science, Hokkaido University, Sapporo 060-0810, Japan*

Received June 19, 2000; in revised form August 14, 2000; accepted October 3, 2000; published online December 21, 2000

Electron paramagnetic resonance (EPR) spectra of tetravalent praseodymium ions doped in the cubic perovskite compound BaHfO<sub>3</sub> have been measured at 4.2 K. A very large hyperfine interaction with the <sup>141</sup>Pr nucleus was observed in the spectrum of Pr<sup>4+</sup>/BaHfO<sub>3</sub>. The results were analyzed based on the weak field approximation, and the *g* value ( $|g| = 0.619$ ) and a hyperfine coupling constant ( $A = 0.0589 \text{ cm}^{-1}$ ) were obtained. The measured *g* value is much smaller than  $|\frac{10}{7}|$ , which indicates that the crystal field effect on the behavior of a 4*f* electron is large. These *g* and *A* values were compared with the EPR results for other *f*<sup>1</sup> ions in an octahedral crystal field.

© 2001 Academic Press

## INTRODUCTION

The most stable oxidation state of lanthanide elements is trivalent. In addition to this state, cerium, praseodymium, and terbium have the tetravalent state (1).

As for magnetic properties, the Pr<sup>4+</sup> and Tb<sup>4+</sup> ions are paramagnetic. We have paid our attention on the Pr<sup>4+</sup> ions in solids. The electronic configuration of the Pr<sup>4+</sup> ion is [Xe]4*f*<sup>1</sup> ([Xe], xenon electronic core). For electronic structure analysis, this *f*<sup>1</sup> configuration is straightforward as only the crystal field and spin-orbit coupling interaction are important. Especially when this ion is located in an octahedral crystal field environment, such a compound is suitable for studying the behavior of 4*f* electron in solids because it is easy to compare the experimental results with theoretical calculation.

Perovskite-type oxides, ABO<sub>3</sub>, where A is a divalent ion (e.g., Sr, Ba) accommodate tetravalent metal ions at the B site of the crystal (2). Figure 1 shows the cubic perovskite-type structure. In an earlier study (3), we successfully measured for the first time the EPR spectrum of the Pr<sup>4+</sup> ion in an octahedral crystal field by doping it in the perovskite BaCeO<sub>3</sub> (where the Pr<sup>4+</sup> ion is substituted for the Ce<sup>4+</sup> ion) and lowering the temperature down to liquid helium temperature. In the EPR spectrum, a very large hyperfine interaction with the <sup>141</sup>Pr nucleus (nuclear spin  $I = \frac{5}{2}$ ) was

measured, and the results could be analyzed based on an octahedral crystal field around the Pr<sup>4+</sup> ion (3). The measured  $|g|$  values are much smaller than  $|\frac{10}{7}|$ , which shows that the crystal field effect on the behavior of a 4*f* electron is large.

In this study, we tried to incorporate the Pr<sup>4+</sup> ions into the Hf site of the cubic perovskite-type compound BaHfO<sub>3</sub>. Through their EPR measurements, we have studied the electronic states of these ions in solids in order to elucidate the behavior of 4*f* electrons which characterize the lanthanide elements. The results for the Pr<sup>4+</sup> ion doped in the BaHfO<sub>3</sub> were compared with those for the Pr<sup>4+</sup>/BaSnO<sub>3</sub> and Pr<sup>4+</sup>/BaZrO<sub>3</sub>, and those for the 5*f*<sup>1</sup> ions in an octahedral crystal field.

## EXPERIMENTAL

### 1. Sample Preparation

Barium carbonate BaCO<sub>3</sub>, praseodymium oxide Pr<sub>6</sub>O<sub>11</sub>, and hafnium metal Hf were used as starting materials. Before use, Pr<sub>6</sub>O<sub>11</sub> was heated in air at 850°C to remove any moisture and to oxidize them to the stoichiometric compositions. They were weighed in the correct metal ratio (BaPr<sub>0.02</sub>Hf<sub>0.98</sub>O<sub>3</sub>), intimately mixed, pressed into pellets, and heated in a flowing oxygen atmosphere at 1300°C in an SiC resistance furnace for 12 h. After cooling to room temperature, the samples were crushed into powder, reground, repressed into pellets, and heated under the same conditions to make the reaction complete. Since these oxides may lose a few oxygen atoms at high temperatures, the samples were kept at 1000°C for 10 h and cooled to room temperature in the furnace so as to prepare oxygen stoichiometric compounds.

### 2. Analysis

An X-ray diffraction analysis was performed with CuK $\alpha$  radiation on a RINT2000 diffractometer (Rigaku) equipped with a curved graphite monochromator.

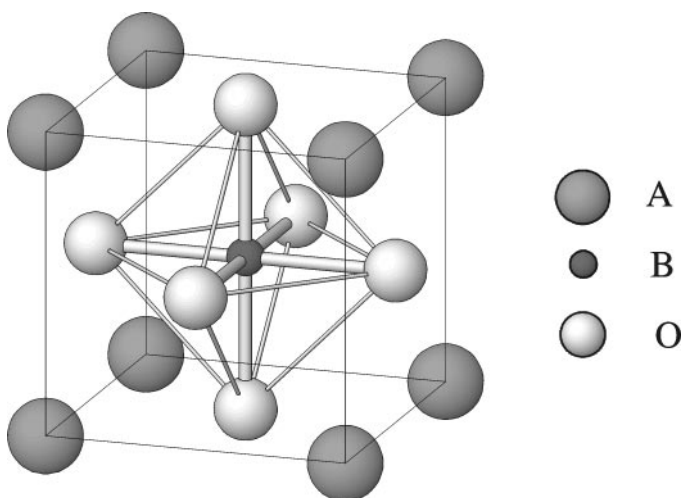


FIG. 1. Crystal structure of cubic perovskite  $ABO_3$ .

### 3. Electron Paramagnetic Resonance Measurement

The EPR spectra at X band ( $\sim 9$  GHz) were measured using a JEOL RE-2X spectrometer operating with an Air Products Helitran cooling system. The magnetic field was swept from 100 to 13,500 G, which was monitored with a proton NMR gaussmeter, and the microwave frequency was measured with a frequency counter. Before the samples were measured, a blank was recorded to eliminate the possibility of interference by the background resonance of the cavity and/or the sample tube.

## RESULTS AND DISCUSSION

The EPR spectra could be measured for the praseodymium ions doped in the  $BaHfO_3$ . With increasing temperature, all the assigned absorption EPR lines become considerably weaker in intensity. This observation strongly indicates that the praseodymium ions are not in the trivalent state, but in the tetravalent state, because the non-Kramers  $Pr^{3+}$  ion usually shows no EPR spectrum (5).

Figure 2 shows the EPR spectra for the  $Pr^{4+}$  ions doped in  $BaHfO_3$  measured at 4.2 K. The observed spectra are composed of five strong absorption lines. We have analyzed the spectrum for the case of  $Pr^{4+}/BaCeO_3$ , in which six absorption lines due to allowed transitions are observed, along with five weaker absorption lines due to forbidden transitions (3). In the present host material, no EPR absorption lines due to forbidden transitions are observed. The number of the measured EPR absorption lines due to the hyperfine interaction with the nuclear spin for  $^{141}Pr$  ( $I = \frac{5}{2}$ ) is not six but five in the experimental field range, which will be discussed later.

The tetravalent praseodymium  $Pr^{4+}$  is a Kramers' ion with one unpaired  $4f$  electron and in a magnetic field one

isotropic EPR spectrum may be observable. The isotope  $^{141}Pr$  (natural abundance 100%) has a nuclear spin of  $I = \frac{5}{2}$  and a nuclear magnetic moment of +4.3 nuclear magnetons. The spin Hamiltonian for the EPR spectrum of  $Pr^{4+}$  ion is

$$H = g\beta\mathbf{H}\cdot\mathbf{S}' + AS'\cdot\mathbf{I} - g'_N\beta\mathbf{H}\cdot\mathbf{I}, \quad [1]$$

where  $g$  is the  $g$  value for  $Pr^{4+}$  with an effective spin  $S' = \frac{1}{2}$ ,  $A$  is the hyperfine coupling constant,  $g'_N$  is the effective nuclear  $g$  value (in units of Bohr magnetons),  $\beta$  is the Bohr magneton, and  $\mathbf{H}$  is the applied magnetic field. Usually the assumption can be made that the electronic Zeeman term (the first term on the right-hand side of Eq. [1]) is much larger than the hyperfine term (the second term on the right-hand side), which would result in a six-line spectrum for an isotropic resonance with  $I = \frac{5}{2}$ . The spacings between them are large enough and they become wider with resonance magnetic field, which indicates that electron spin quantum number ( $m_s$ ) and nuclear spin quantum number ( $m_I$ ) are not good (pure) quantum numbers. We have to solve the Hamiltonian [1] exactly. The solution has been given by Ramsey (6) and others (7).

First,  $I$  and  $S$  are coupled together to form the resultant  $F$ , where  $F = I + S$ . For  $S = \frac{1}{2}$  and  $I = \frac{5}{2}$  in the absence of a magnetic field, there are two states,  $F = 2$  and  $F = 3$ , which are separated by  $3A$ . When the magnetic field is included, each of these two states splits into  $(2F + 1)$   $|m_F\rangle$  Zeeman levels and six allowed transitions ( $\Delta F = 0, \pm 1; \Delta m_F = \pm 1$ ) are observable as shown in Fig. 3.

By fitting the observed EPR spectra for  $Pr^{4+}/BaHfO_3$  to the parameters of the spin Hamiltonian [1], the best fit parameters  $g$  and  $A$  are obtained;  $|g| = 0.619$ ,  $|A| = 0.0589 \text{ cm}^{-1}$ , and the calculation results are shown in Table 1. They show that the resonance field for the sixth allowed transition is 15,034 G, which is beyond our maximum magnetic field. Figure 3 shows the Zeeman energy levels calculated for  $Pr^{4+}$  in  $BaHfO_3$ . Arrows show the observable EPR transitions.

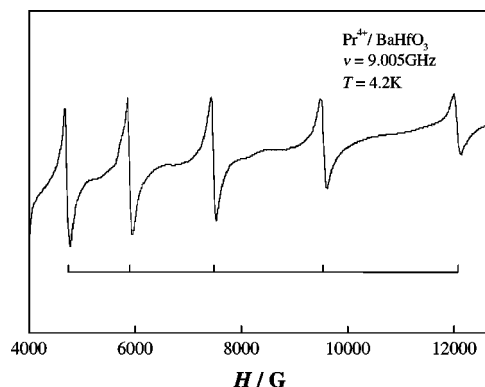


FIG. 2. EPR spectrum for  $Pr^{4+}$  doped in  $BaHfO_3$  measured at 4.2 K. Isotropic EPR absorption line positions are depicted with the stick diagram below.

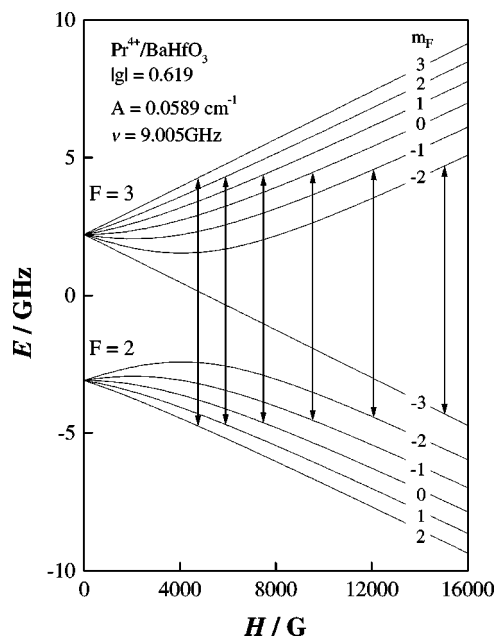


FIG. 3. Zeeman energy levels of Pr<sup>4+</sup> in BaHfO<sub>3</sub>. Arrows show the observable EPR transitions at 4.2 K.

Although the sign of the  $g$  value is not obtained by this experiment, comparison with other  $f^1$  system in octahedral symmetry, such as NpF<sub>6</sub>/UF<sub>6</sub> (8) and Pa<sup>4+</sup>/Cs<sub>2</sub>ZrCl<sub>6</sub> (7), where the sign of the  $g$  value has been measured, indicates that the  $g$  value for the Pr<sup>4+</sup> ion doped in the perovskite-type compound should be also negative.

We will discuss the  $g$  value determined in this experiment. The Pr<sup>4+</sup> ion is substituted for the Hf<sup>4+</sup> ion and it is octahedrally coordinated by six oxygen ions. For one  $f$  electron, the <sup>2</sup>F Russell-Saunders state breaks up into two  $J$  states,  $J = \frac{5}{2}$  and  $J = \frac{7}{2}$ , when the effect of spin-orbit coupling is included. The excited state <sup>2</sup>F<sub>7/2</sub> lies above the ground state <sup>2</sup>F<sub>5/2</sub> by the energy  $\frac{7}{2}\zeta$  ( $\zeta$ : the spin-orbit coupling constant). When the crystal field with an octahedral

symmetry is taken into account, the  $J = \frac{5}{2}$  state breaks up into a doubly degenerate  $\Gamma_7$  state and a fourfold degenerate  $\Gamma_8$  state. The higher-lying  $J = \frac{7}{2}$  state breaks up into two doubly degenerate states,  $\Gamma_6$  and  $\Gamma_7'$ , and a fourfold degenerate  $\Gamma_8'$  state (9). Figure 4 shows the relative energy level splittings of an  $f^1$  electron in octahedral symmetry. In the absence of spin-orbit coupling, i.e., in the strong crystal field limit, the energy level separations are  $\Delta = E(\Gamma_5) - E(\Gamma_2)$  and  $\theta = E(\Gamma_4) - E(\Gamma_5)$ . The ground state in this symmetry is the  $J = \frac{5}{2}$ ,  $\Gamma_7$  state. The  $g$  value for the  $\Gamma_7$  ground doublet in a pure  $J = \frac{5}{2}$  manifold would be  $-\frac{5}{3}$  times the Landé  $g$  factor. Since the Landé factor for the  $f^1$  configuration is equal to  $\frac{6}{7}$ , the  $g$  value is  $-\frac{10}{7}$ . When the crystal field interaction is not small compared to the spin-orbit coupling interaction, the excited  $J = \frac{7}{2}$ ,  $\Gamma_7'$  state is mixed into the ground  $J = \frac{5}{2}$ ,  $\Gamma_7$  state via this interaction. The resulting expression for the ground state  $g$  value is given by

$$g = -2\left(\frac{5}{7}\cos^2\alpha - \frac{8}{21}\sqrt{3}\cos\alpha\sin\alpha - \frac{12}{7}\sin^2\alpha\right), \quad [2]$$

with

$$|\Gamma_7\rangle = \cos\alpha|J = \frac{5}{2}, \Gamma_7\rangle - \sin\alpha|J = \frac{7}{2}, \Gamma_7'\rangle. \quad [3]$$

The parameter  $\alpha$  in Eq. [2] is related to  $\Delta$  and  $\zeta$  by the following expression

$$\tan\alpha = \frac{2\sqrt{3}}{7} \frac{\Delta}{\frac{7}{4}\zeta - \frac{1}{14}\Delta + \frac{1}{2}\sqrt{\left(\frac{7}{2}\zeta\right)^2 - \Delta\zeta + \Delta^2}}. \quad [4]$$

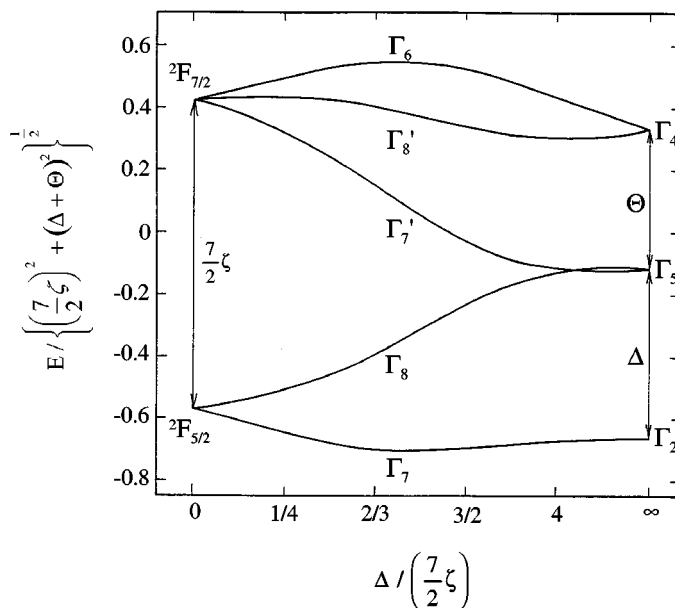


FIG. 4. Relative energy splitting of an  $f^1$  electron as the relative magnitudes of the crystal field (with octahedral symmetry) and spin-orbit coupling interactions ( $\Delta/(\frac{7}{2}\zeta)$ ) change.

TABLE 1

Experimental and Calculated EPR Absorption Line Positions for Pr<sup>4+</sup>/BaHfO<sub>3</sub>

$H_{\text{exp}}(\text{G})$	$H_{\text{cal}}(\text{G})$	$H_{\text{differ}}(\text{G})$
4,742	4,742	0
5,899	5,903	-4
7,484	7,477	7
9,532	9,535	-3
12,078	12,077	1
—	15,034	—

$|g|$  0.619  
 $A$  0.0589 cm<sup>-1</sup>

Note.  $g_N$  set to equal to 0.0.

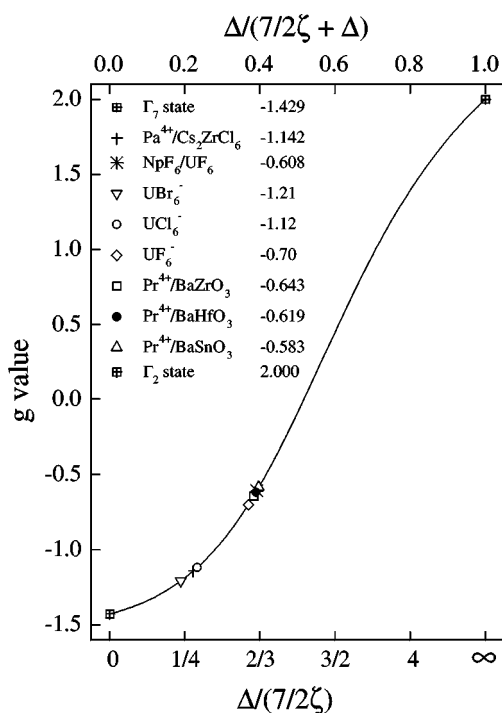


FIG. 5.  $g$  Value vs the ratio  $\Delta/(\frac{7}{2}\zeta)$  for a number of  $f^1$  compounds in octahedral symmetry.

Figure 5 shows the variation of the  $g$  value for an  $f^1$  configuration in octahedral symmetry against the relative strength of the crystal field to the spin-orbit splitting,  $\Delta/(\frac{7}{2}\zeta)$ . With increasing admixture (i.e., increasing crystal field strength), the  $g$  value becomes larger, but can never exceed two (3). The  $|g|$  value obtained here is smaller than  $|\frac{10}{7}|$ , which indicates that the crystal field is effective on the behavior of a  $4f$  electron in this compound.

Since the  $g$  value for an  $f$  electron in octahedral symmetry is negative, the value of  $|g|$  which is obtained from this EPR experiment should decrease with increasing crystal field strength. Previously, we have measured the EPR spectra for the  $\text{Pr}^{4+}$  ions in the cubic  $\text{BaZrO}_3$  and  $\text{BaSnO}_3$  which are isomorphous with  $\text{BaHfO}_3$ . Their  $|g|$  values and hyperfine coupling constants  $A$  are as follows:  $|g| = 0.643$  and  $|A| = 0.0597 \text{ cm}^{-1}$  for  $\text{Pr}^{4+}/\text{BaZrO}_3$ , and  $|g| = 0.583$  and

$|A| = 0.0589 \text{ cm}^{-1}$  for  $\text{Pr}^{4+}/\text{BaSnO}_3$  (10). The lattice parameters for  $\text{BaPr}_{0.02}\text{Zr}_{0.98}\text{O}_3$ ,  $\text{BaPr}_{0.02}\text{Hf}_{0.98}\text{O}_3$ , and  $\text{BaPr}_{0.02}\text{Sn}_{0.98}\text{O}_3$  are 4.1987, 4.1750, and 4.1239 Å, respectively. With shrinking of the lattice ( $\text{BaZrO}_3 \rightarrow \text{BaHfO}_3 \rightarrow \text{BaSnO}_3$ ), the  $|g|$  value decreases. This is due to the increase of the crystal field strength by the shrinkage of the lattice, which is consistent with the above discussion. In Fig. 5, the  $g$  values for the  $5f^1$  ions (7, 8, 11–13) are also shown. They vary from  $-1.142$  for  $\text{Pa}^{4+}/\text{Cs}_2\text{ZrCl}_6$  (weak crystal field, (7)) to  $-0.608$  for  $\text{NpF}_6/\text{UF}_6$  (strong crystal field, (8)). The measured  $g$  value for  $\text{Pr}^{4+}/\text{BaHfO}_3$  is comparable to the magnitude of the  $g$  value for  $\text{NpF}_6/\text{UF}_6$ ; i.e., the effect of the crystal field in the  $\text{Pr}^{4+}/\text{BaHfO}_3$  is as large as that in  $\text{NpF}_6/\text{UF}_6$ .

#### ACKNOWLEDGMENT

This work was supported by a Grant-in-Aid for Scientific Research on Priority Areas "Novel Quantum Phenomena in Transition Metal Oxides-Spin Charge Orbital Coupled Systems," No. 12046203, from the Ministry of Education, Science, Sports, and Culture of Japan.

#### REFERENCES

1. N. E. Topp, in "Chemistry of the Rare-Earth Elements." Elsevier, Amsterdam, 1965.
2. J. B. Goodenough and J. M. Longo, in "Landolt-Börnstein Tabellen" (K.-H. Hellwege and A. M. Hellwege, Eds.), Neue Serie, III Band, 4a, Chap. 3. Springer-Verlag, Berlin, 1970.
3. Y. Hinatsu and N. Edelstein, *J. Solid State Chem.* **112**, 53 (1994).
4. J. M. Baker, J. R. Chadwick, G. Garton, and J. P. Hurrell, *Proc. R. Soc. A* **286**, 352 (1965).
5. A. Abragam and B. Bleaney, in "Electron Paramagnetic Resonance of Transition Ions." Oxford Univ. Press, London, 1970.
6. N. F. Ramsey, in "Molecular Beams." Clarendon Press, Oxford, 1956.
7. J. D. Axe, H. J. Stapleton, and C. D. Jeffries, *Phys. Rev.* **121**, 1630 (1961).
8. C. A. Hutchison and B. Weinstock, *J. Phys. Chem.* **32**, 56 (1960).
9. B. R. Judd, in "Operator Techniques in Atomic Spectroscopy." McGraw-Hill, New York, 1963.
10. Y. Hinatsu, T. Fujino, and N. Edelstein, *J. Solid State Chem.* **99**, 182 (1992).
11. P. Rigny and P. Plurien, *J. Phys. Chem. Solids* **32**, 1175 (1967).
12. J. Selbin, J. D. Ortego, and G. Gritzner, *Inorg. Chem.* **7**, 976 (1968).
13. J. Selbin, C. Ballhausen, and D. G. Durrett, *Inorg. Chem.* **11**, 510 (1972).